

# Publications with LPKF Equipment, Part 1

Selection of internationally published scientific articles using LPKF equipment

February 2021



## TOC: page, system, application

**3** [PL U4: Flex electrodes for pacemaker](#)

**4** [PL U4: Implantable flex board](#)

**5** [PL U4: Wireless flex flow sensor](#)

**6** [PL U4: MW sensor for blood sugar measurement](#)

**7** [PL U3: Specular reflection absorber](#)

**8** [PL U: Atmospheric pressure plasma jets](#)

**9** [PL 200: Optical signal routing using Hall effect](#)

**10** [PM H100: Planar Antenna](#)

**11** [PM S103: RF tunable Quad-band filter](#)

**12** [PM S103: Robotic hand prosthesis](#)

**13** [PM S63: Reconfigurable Antennas](#)

**14** [PM S100: Wearable microfluidic sensor](#)

**15** [PM C100: High gain low noise amplifier](#)

**16** [PM E33: CPW-fed antenna for Ku-Band](#)

**17** [PM E33: Low-profile antenna for Ku-Band](#)

**18** [PF S: Printed antenna for wearables](#)

## Wireless, battery-free, fully implantable multimodal and multisite pacemakers for applications in small animal models

Small animals support a wide range of pathological phenotypes and genotypes as versatile, affordable models for pathogenesis of cardiovascular diseases and for exploration of strategies in electrotherapy, gene therapy, and optogenetics. Pacing tools in such contexts are currently limited to tethered embodiments that constrain animal behaviors and experimental designs. Here, we introduce a highly miniaturized wireless energy-harvesting and digital communication electronics for thin, miniaturized pacing platforms weighing 110 mg with capabilities for subdermal implantation and tolerance to over 200,000 multiaxial cycles of strain without degradation in electrical or ...

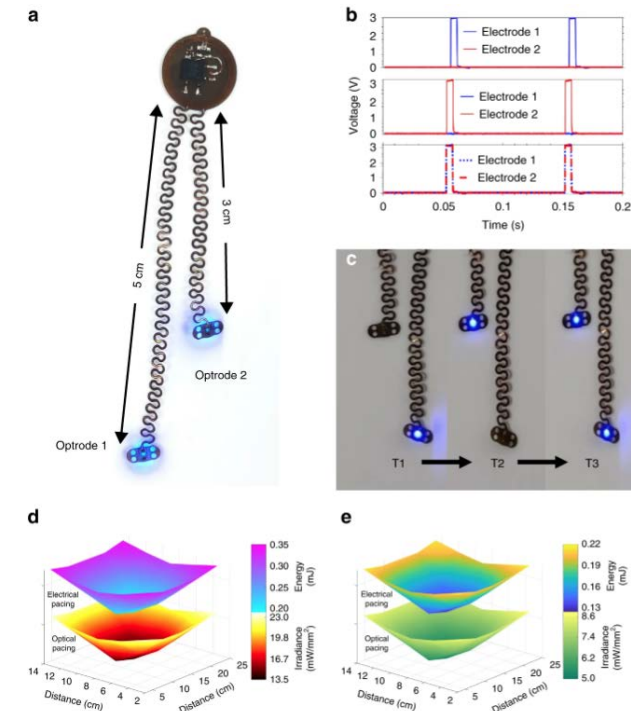
### Device fabrication

Pyralux AP8535R served as a substrate for the circuit, the serpentine interconnect and the optrode. The top and bottom copper layers (17.5  $\mu\text{m}$  thick) and via holes were structured via direct laser ablation (LPKF U4). Through-hole plating was performed via pulsed direct current electroplating of copper (LPKF Contac U4), to define the electrical connections between the top and bottom layers. Electron beam evaporation of 200 nm platinum defines the electrode surface.

Department of Biomedical Engineering, University of Arizona, Tucson, AZ, 85721, USA

<https://www.nature.com/articles/s41467-019-13637-w>

wireless, battery-free, fully implantable



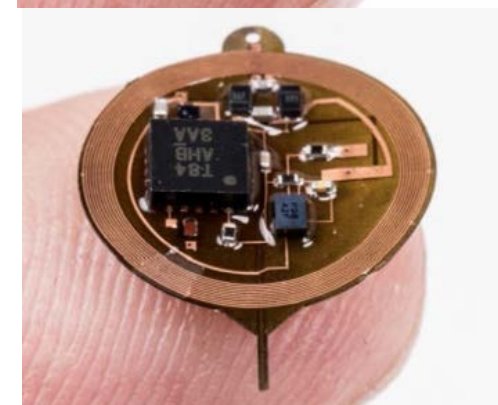
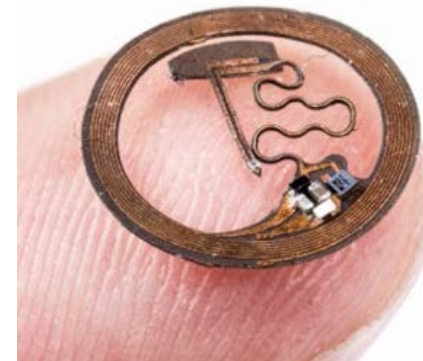
## Fully implantable optoelectronic systems for battery-free, multimodal operation in neuroscience research

Recently developed ultrasmall, fully implantable devices for optogenetic neuromodulation eliminate the physical tethers associated with conventional set-ups and avoid the bulky head-stages and batteries found in alternative wireless technologies. The resulting systems allow behavioural studies without motion constraints and enable experiments in a range of environments and contexts, such as social interactions. However, these devices are purely passive in their electronic design, thereby precluding any form of active control or programmability; independent operation of multiple devices, or of multiple active components in a single device, is, in particular, impossible.

### Device fabrication

Pyralux AP8535R served as a substrate for the flex circuit. The top and bottom copper layers (17.5  $\mu$  m thick) were structured via direct laser ablation (LPKF U4). Through hole plating via pulsed direct current electroplating of copper (LPKF Contac S4) defined the electrical connections between the top and bottom layers. Components with commercial packaging were attached via reflow soldering with low-temperature solder (IndiumCorp). The  $\mu$ -ILEDs were mounted with a pick-and-place tool (Finetech Fineplacer pico ma) using defined force and temperature (180 °C) with an anisotropic...

battery-free, fully implantable,  
ultrasmall,



Center for Bio-Integrated Electronics at the Simpson Querrey Institute for BioNanotechnology and the Department of Materials Science and Engineering, Northwestern University, Evanston, IL, USA

<https://www.nature.com/articles/s41928-018-0175-0>



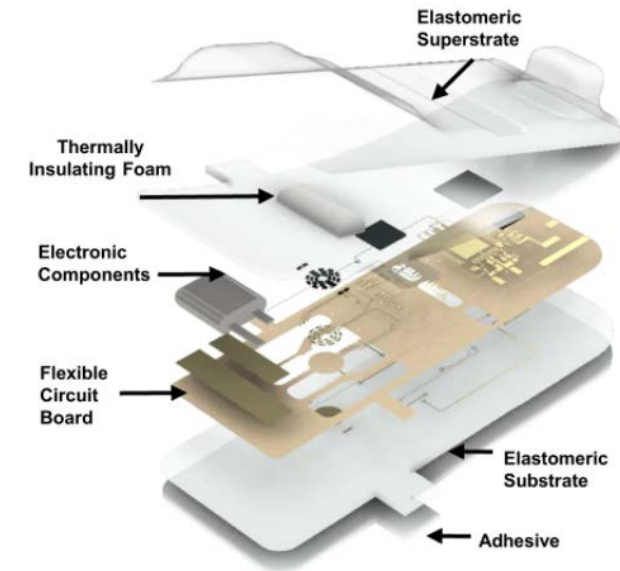
## Continuous, noninvasive wireless monitoring of flow of cerebrospinal fluid through shunts in patients with hydrocephalus

Hydrocephalus is a common disorder caused by the buildup of cerebrospinal fluid (CSF) in the brain. Treatment typically involves the surgical implantation of a pressure-regulated silicone tube assembly, known as a shunt. Unfortunately, shunts have extremely high failure rates and diagnosing shunt malfunction is challenging due to a combination of vague symptoms and a lack of a convenient means to monitor flow. Here, we introduce a wireless, wearable device that enables precise measurements of CSF flow, continuously or intermittently, in hospitals, laboratories or even in home settings. The technology exploits measurements of thermal transport...

### Fabrication and assembly of electronics

Fabrication of the sensor and supporting electronics began with processing of a trilayer film of copper/PI/copper (18  $\mu\text{m}$ /75  $\mu\text{m}$ /18  $\mu\text{m}$ , Pyralux, DuPont Inc.) with a UV laser cutter (LPKF U4) to pattern traces, bond pads, and unplated vias. Successive washes in stainless steel flux (Worthington Inc), deionized water, and isopropanol (Fisher Scientific) removed surface oxides and prepared the resulting flexible PCB (fPCB) for assembly. Reflow soldering with low-temperature solder paste (TS391LT, ChipQuik) established electrical contacts between commercial-off-the-shelf components...

wearable device, wireless,,  
continuous flow monitoring



Department of Materials Science and Engineering, Frederick Seitz Materials Research Laboratory, University of Illinois at Urbana-Champaign, Urbana, IL, 61801, USA

<https://www.nature.com/articles/s41746-020-0239-1>



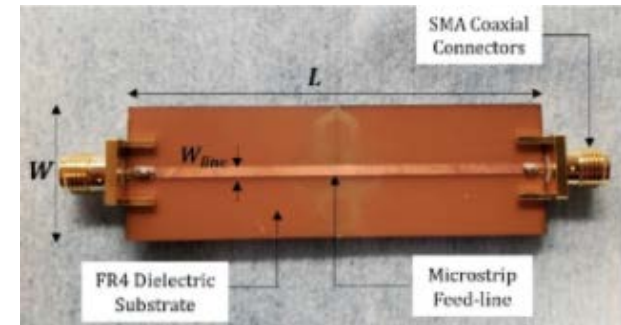
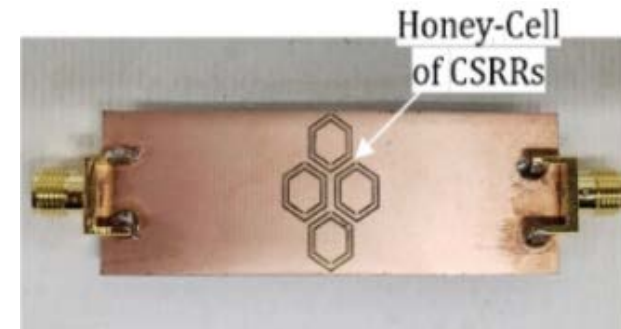
## Low-cost portable microwave sensor for non-invasive monitoring of blood glucose level: novel design utilizing a four-cell CSRR hexagonal configuration

This article presents a novel design of portable planar microwave sensor for fast, accurate, and non-invasive monitoring of the blood glucose level as an effective technique for diabetes control and prevention. The proposed sensor design incorporates four cells of hexagonal-shaped complementary split ring resonators (CSRRs), arranged in a honey-cell configuration, and fabricated on a thin sheet of an FR4 dielectric substrate. The CSRR sensing elements are coupled via a planar microstrip-line to a radar board operating in the ISM band 2.4–2.5 GHz. The integrated sensor shows an impressive detection capability and a remarkable sensitivity of blood glucose levels (BGLs).

### Sensor fabrication

The sensor prototype was fabricated on an FR4 PCB of a copper thickness of 35  $\mu\text{m}$  and dielectric substrate of 0.8 mm thickness using the laser technology incorporated in the proto-laser machine (LPKF ProtoLaser U4). First, the DipTracer PCB layout software was used to generate the Gerber files (.gbr) from the DXF HFSS design files for the CSRR structure. A few fiducial points were added to the design to ease the alignment of top and bottom parts in fabrication. The CircuitPro software was used to control the laser micromachining when fabricating the CSRR device. On the top layer of...

Microwave sensor, blood glucose measurement, non-invasive monitoring



Department of Electrical and Computer Engineering, Centre for Intelligent Antenna and Radio Systems (CIARS), University of Waterloo, Waterloo, ON, Canada

<https://www.nature.com/articles/s41598-020-72114-3>



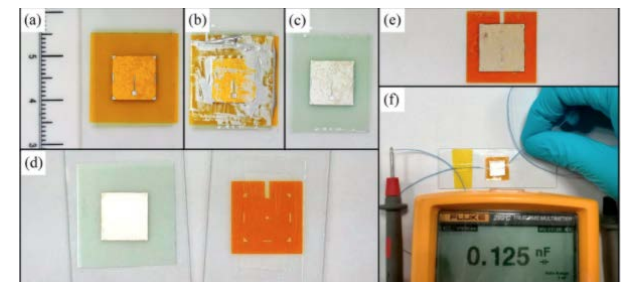
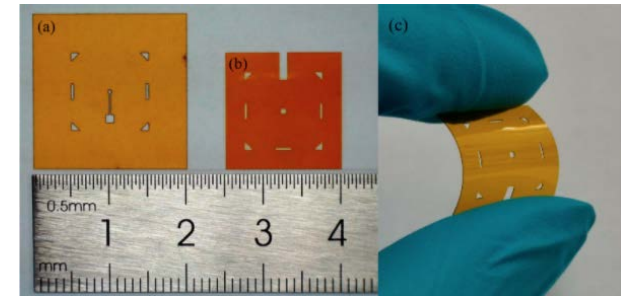
## Low Temperature Adhesive Bonding-Based Fabrication of an Air-Borne Flexible Piezoelectric Micromachined Ultrasonic Transducer

This paper presents the development of a flexible piezoelectric micromachined ultrasonic transducer (PMUT) that can conform to flat, concave, and convex surfaces and work in air. The PMUT consists of an Ag-coated polyvinylidene fluoride (PVDF) film mounted onto a laser-manipulated polymer substrate. A low temperature (<math><100\text{ }^\circ\text{C}</math>) adhesive bonding technique is adopted in the fabrication process. Finite element analysis (FEA) is implemented to confirm the capability of predicting the resonant frequency of composite diaphragms and optimizing the device. The manufactured PMUT exhibits a center frequency of 198 kHz with a wide operational bandwidth. Its acoustic ...

### Fabrication Process

The low temperature adhesive bonding fabrication process is divided into pre-processing and main processing steps. A laser precision machining system (ProtoLaser U3, LPKF Tianjin Co., Ltd., Tianjin, China) is used to quickly pattern printing masks and flexible substrates in pre-processing. Compared with micromachining fabrication techniques such as standard photolithography, depositing, and etching, laser precision machining is convenient and time-saving. The diameter of focused laser beam is 30  $\mu\text{m}$ , and the minimum space of ultra-fine structures can reach 45  $\mu\text{m}$ , which will ....

Wearable devices, piezoelectric transducer, Kapton stencil



State Key Laboratory of Mechanics and Control of Mechanical Structures, Nanjing University of Aeronautics

<https://www.mdpi.com/1424-8220/20/11/3333/htm>



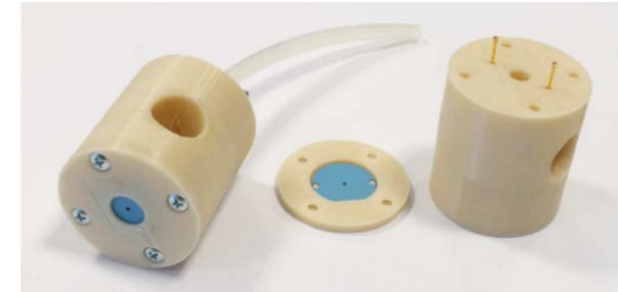
## Plasma Jets Fabricated in Low-Temperature Cofired Ceramics for Gold Nanoparticles Synthesis

In this article, we present a development of atmospheric pressure plasma jets (APPJs) for modification of liquid solutions. APPJs were fabricated in low temperature cofired ceramics (LTCC) technology. During the measurements, plasma jets worked under various flowing gases, which can be used to produce plasma activated water. In addition, owing to the plasma treatment, it was possible to decrease the time of a synthesis of gold nanoparticles (AuNPs) without the use of additional hazardous reagents. The mechanism of gold nanoparticles formation in cold nitrogen plasma is also presented.

### Fabrication

Ceramic structures were made of LTCC DuPont 951 (DuPont, Wilmington, NC, USA) ceramics and compatible pastes. The thickness of the ceramic foil used depended on the height of the recess and the thickness of the dielectric layers of the structure. The pattern of each layer was laser-cut using LPKF Proto Laser U (LPKF, Garbsen, Germany). Metal layers were screen-printed using Aurel vs. 1520A (Aurel Automation SPA, Modigliana FC, Italy). All the layers were laminated for 20 min under 20 MPa pressure in the isostatic press and then green plasma jets were fired in a typical LTCC ...

atmospheric pressure plasma jets, low temperature cofired ceramics, gold nanoparticles synthesis



Faculty of Microsystem Electronics and Photonics, Wrocław University of Science and Technology, 50-370 Wrocław, Poland

<https://www.mdpi.com/1996-1944/13/14/3191/htm>

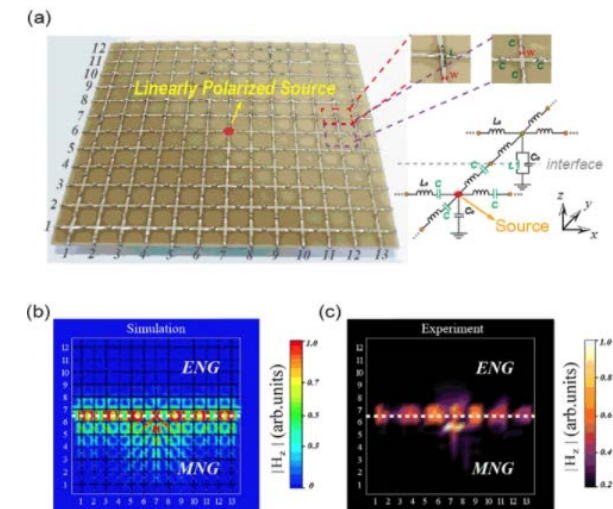
## Photonic Spin Hall Effect in Waveguides Composed of Two Types of Single-Negative Metamaterials

The polarization controlled optical signal routing has many important applications in photonics such as polarization beam splitter. By using two-dimensional transmission lines with lumped elements, we experimentally demonstrate the selective excitation of guided modes in waveguides composed of two kinds of single-negative metamaterials. A localized, circularly polarized emitter placed near the interface of the two kinds of single-negative metamaterials only couples with one guided mode with a specific propagating direction determined by the polarization handedness of the source. Moreover, this optical spin-orbit locking phenomenon, also called the photonic spin Hall effect, ...

### Methods

A commercial software package (CST Microwave Studio) is used in designing the samples. The samples are all fabricated on copper-clad 1.6 mm thick FR4 substrates using laser direct structuring technology (LPKF ProtoLaser 200). In the experiment, the signal emission from the port one of vector network analyzer (Agilent PNA Network Analyzer N5222A) and another antenna (i.e., near-filed probe) connecting to the port 2 of analyzer are employed to measure the magnetic fields. A circular probe is vertically placed 1mm above the TLs to measure the signals of magnetic field of ...

optical signal routing, metamaterials, photonic spin Hall effect



Key Laboratory of Advanced Micro-structure Materials, MOE, School of Physics Science and Engineering, Tongji University, Shanghai, 200092, China

<https://www.nature.com/articles/s41598-017-08171-y>



## Mutual Coupling Reduction between Finite Spaced Planar Antenna Elements Using Modified Ground Structure

In this paper, a modified ground structure capable of reducing mutual coupling to provide isolation between adjacent antenna elements is presented. The proposed modified ground structure is a combination of a strategically located ground slot, asymmetric partial ground and a substrate-integrated pin wall. The use of the modified ground structure causes a more than 28 dB (measured value) mutual coupling reduction. The modified ground structure has been optimized and validated with a finite spaced planar  $2 \times 1$  antenna array operating at 4.16 GHz, intended for unmanned aerial vehicle radar altimeter applications.

For the **fabrication**, the LPKF ProtoMat H100 was used. In the first step, metallic traces were milled on RT duroid 5880 substrate. In the next step, a drilling bit with a diameter of 0.4 mm was used to create holes through the substrate. Since the required substrate thickness of 4.71 mm (S3) was not available as a standard thickness of RT duroid boards, three substrate sheets with thickness 1.57 mm were stacked together while the 0.4 mm holes were aligned. Copper wires of diameter 0.36 mm were passed through the aligned sheets via holes to finally develop the substrate-integrated pin wall as shown in [Figure 5a](#).

School of Electronic and Information Engineering, Beihang University, Beijing 100191, China

<https://www.mdpi.com/2079-9292/10/1/19/htm>

mutual coupling reduction; altimeter; antenna array; modified ground structure

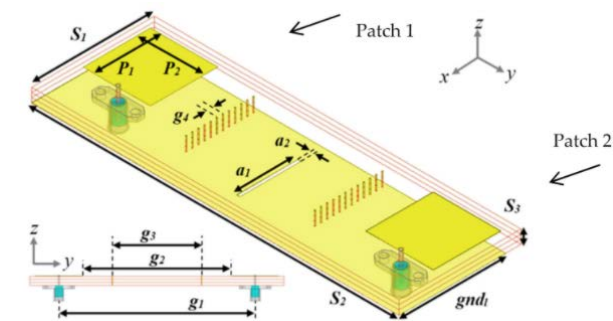
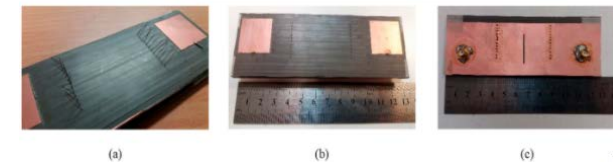


**Figure 5.** Fabricated prototype of the proposed antenna array: (a) Intermediate step while developing the substrate-integrated pin wall; (b) Front view; (c) Back view.



## Design and implementation of magnetically-tunable quad-band filter utilizing split-ring resonators at microwave frequencies

In this article, we present a magnetically-tunable quad-band filter with high tunability in the frequency range of 2.1–3.9 GHz. A multi-band filter with four stop-bands comprises of a microstrip line coupled to four frequency-selective split-ring resonators (SRRs). We achieve tuning of individual frequency bands using magnetic reed switches connected in between the capacitive gaps of each split-ring resonator. Application of magnetic field tunes this capacitance affecting its resonance frequency. The measured reflection spectrum of the proposed device matches well with the simulation results. The results show more than 25% tunability for each of the four bands ...

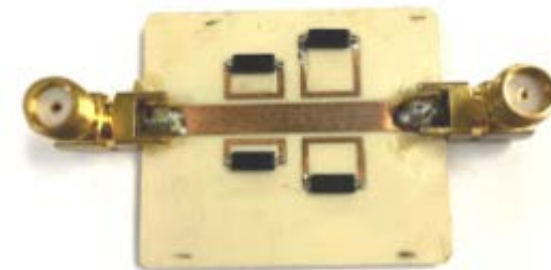
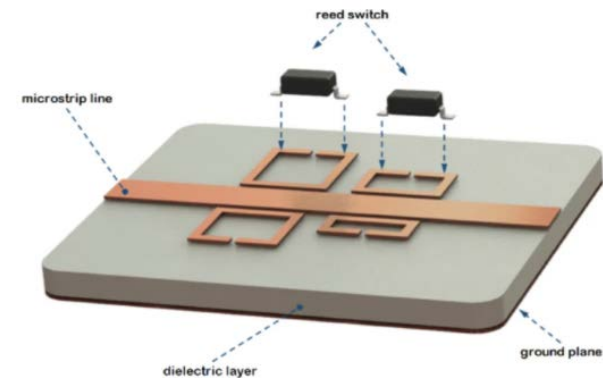
### Experimental Results

Magnetically tunable quad-band microwave filters comprised of a microstrip line, split-ring resonators and reed switches have been implemented on commercially available double-sided Rogers RO4003C high-frequency boards patterned using LPKF Protomat S103 (LPKF Laser & Electronics AG, Garbsen, Germany) with standard printed circuit board (PCB) fabrication methods. After milling the board, magnetic MEMS reed switches (MK24-A-3, a SPST normally open (NO) switch from Standex Electronics, Cincinnati, OH, USA) are soldered in the gap of each individual ...

Nano Lab, Advanced Technology Laboratory, 200 Boston Ave, Medford, MA, 02155, USA

<https://www.nature.com/articles/s41598-020-57773-6>

magnetically-tunable quad-band filter, split-ring resonator



## Development of an EMG Controlled Robotic Hand Prosthesis

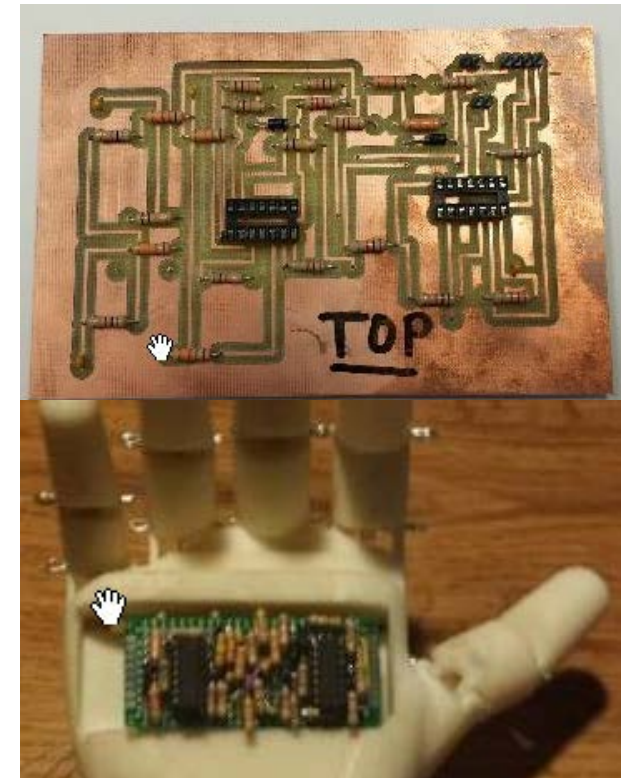
A robotic hand used as a prosthetic can be made using 3D printed material to replicate the normal anatomy and mechanical movement of the human hand using muscle signals associated with human finger movements. EMG electrodes were placed on the flexor carpi radialis, palmaris longus, flexor carpi ulnaris, flexor digitorum superficialis, and flexor pollicis longus to acquire EMG signals during finger movement. Analog integrated circuits were designed to amplify, filter and rectify the muscle signals with 4550 gain, 20-500 Hz cutoff frequencies for second order Butterworth bandpass filter, and a full wave rectifier circuit using LM324 quad operational amplifier.

A printed circuit board was designed using Cadence OrCAD software and PCBMaker. LPKF ProtoMat S103 plotter was used for milling and cutting the PCB board. An Arduino® Micro™ ATmega32U4 8-bit microcontroller board was used to convert analog signals into digital at 10 bits of resolution and generate pulse-width modulation (PWM) signals for servo motors of the 3D printed robotic hand. Siemens NX® 10.0 software was used to create a model for robotic hand and printed it in Stratasys® Dimension Elite 3D printer. The robotic hand was designed to be anatomically similar to the normal hand using anthropometric data. Real time control of an individual finger of the 3D printed robotic hand was achieved through Arduino programming.

Department of Biomedical Engineering, Indiana Institute of Technology, Fort Wayne, IN 46803

[https://www.researchgate.net/publication/315736180\\_Development\\_of\\_an\\_EMG\\_Controlled\\_Robotic\\_Hand\\_Prosthesis](https://www.researchgate.net/publication/315736180_Development_of_an_EMG_Controlled_Robotic_Hand_Prosthesis)

Prosthetic hand, robotic hand



## Characterization of Novel Structures Consisting of Micron-Sized Conductive Particles That Respond to Static Magnetic Field Lines for 4G/5G (Sub-6 GHz) Reconfigurable Antennas

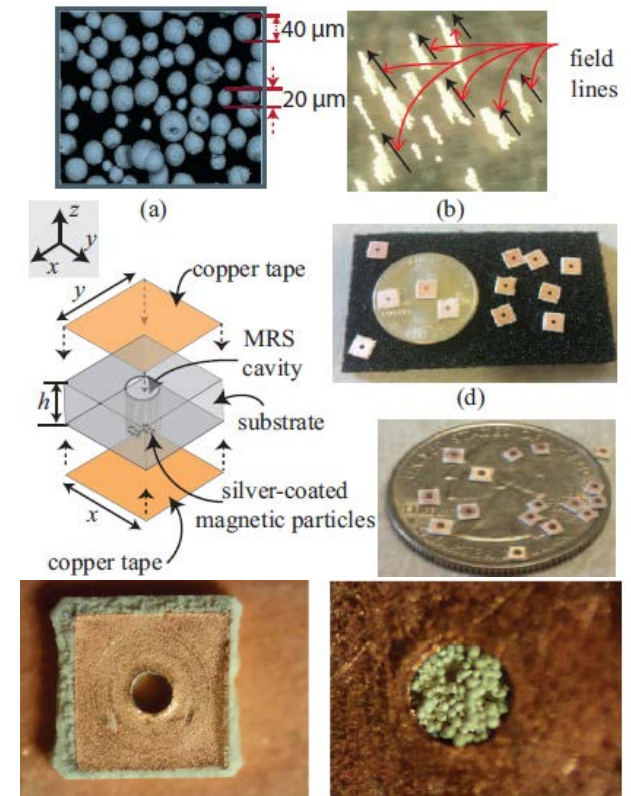
Controlling Radio Frequency (RF) signals through switching technology is of interest to designers of modern wireless platforms such as Advanced Wireless services (AWS) from 2.18 GHz–2.2 GHz, mid-bands of sub-6 GHz 5G (2.5 GHz and 3.5 GHz), and 4G bands around 600 MHz/700 MHz, 1.7 GHz/2.1 GHz/2.3 GHz/2.5 GHz. This is because certain layout efficiencies can be achieved if suitable components are chosen to control these signals. The objective of this paper is to present a new model of an RF switch denoted as a Magnetostatic Responsive Structure (MRS) for achieving reconfigurable operation in 4G/5G antennas.

The **manufacturing** of the MRS was achieved in-house using the LPKF ProtoMat S63 PCB [13] milling machine. In particular, milling practices were used to make the cavities in a substrate and for accurate cutting of the MRSs. Initially, a 0.9 mm cavity diameter  $d$  on a 3.0 mm  $\times$  3.0 mm substrate having a thickness of 0.508 mm  $h$  was accurately manufactured and is shown in Figure 1d. The substrate material used was a Rogers TMM4 with 1 oz. copper cladding on both the top and bottom. This practice validated the feasibility of milling practices and even smaller structures were manufactured using this milling machine process. Figure 1e shows the manufactured MRSs cavities with a diameter of 0.9 mm on a Rogers TMM4 substrate having a size of 1.5 mm  $\times$  1.5 mm  $\times$  0.508 mm.

Department Electrical and Computer Engineering, COMSATS University Islamabad, Islamabad 45550, Pakistan

<https://www.mdpi.com/2079-9292/9/6/903>

### Advanced Wireless services Magnetostatic Responsive Structure



## Monitoring biomolecule concentrations in tissue using a wearable droplet microfluidic-based sensor

Knowing how biomarker levels vary within biological fluids over time can produce valuable insight into tissue physiology and pathology, and could inform personalized clinical treatment. We describe here a wearable sensor for monitoring biomolecule levels that combines continuous fluid sampling with in situ analysis using wet-chemical assays (with the specific assay interchangeable depending on the target biomolecule). The microfluidic device employs a droplet flow regime to maximize the temporal response of the device, using a screw-driven push-pull peristaltic micropump to robustly produce nanolitre-sized droplets. The fully integrated sensor is contained within a small ...

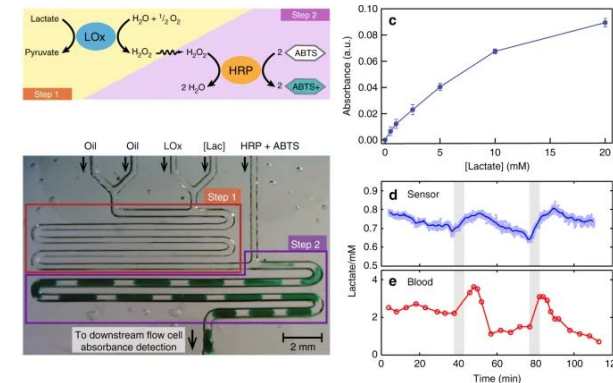
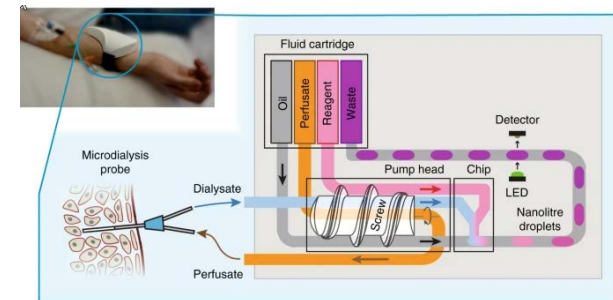
### Flow cell design and setup

The flow cell, shown in Supplementary Fig. 11, was based on a previously reported design<sup>31</sup> and consisted of a black acrylic body which held the optical components and directed the light path through the fluid as it passed through PTFE tubing. The body was micromilled using a LPKF Protomat S100 micromill (LPKF Laser & Electronics Ltd., Berkshire, UK) from two 3 mm-thick black polymethylmethacrylate (PMMA) blocks. A straight centre groove of dimension 1.0 mm by 1.0 mm was milled to take the PTFE tubing. Perpendicular to the groove, a through-hole of square cross-section (0.4 mm) was milled to direct the light path. Recesses at each end of the through-hole ...

Faculty of Engineering and Physical Sciences, University of Southampton, Southampton, SO17 1BJ, UK

<https://www.nature.com/articles/s41467-019-10401-y#MOESM1>

Wearable sensor, microfluidic, in situ analysis, biomarker



## High gain low noise amplifier design used for RF front end application

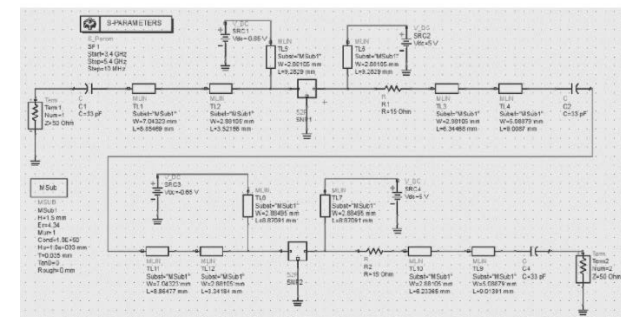
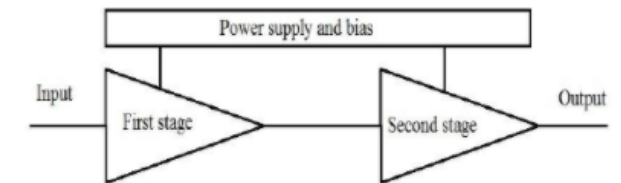
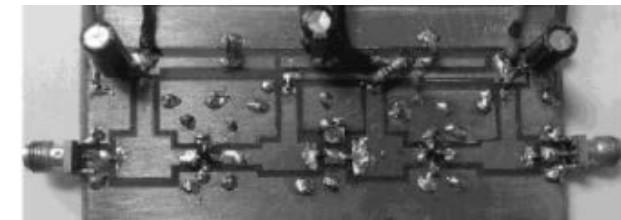
This paper presents the design and fabrication of a wideband low noise amplifier (LNA) at 4 - 5 GHz, which suitable for RF front end application. The design of the LNA uses diagram of two-stage cascade amplifier with different center frequency in order to create a good wideband performance and high gain. The LNA has been fabricated on a PCB board with FR4 substrate using microstrip technology and pHEMT FET transistor amplifier with following specifications: Maximum overall gain of 26.046 dB, operating frequency from 4 GHz to 5 GHz, noise figure is about 1.515 dB, the reverse isolation of -29.5 dB, the LNA using a 5 V supply voltage respectively and total current consumptions of 20 mA. All the designed, simulated and fabricated processes were done using Agilent' ADS 2009 package and machine LPKF Protomat C40.

A two-stage LNA with spf-3043 is designed and demonstrated with simulations in ADS package as well as tuning for the optimum gain, noise figure and bandwidth. The design was fabricated and the board was measured and analyzed together with the simulated results. In summary, the measurement results of the LNB were compared to references with following its performances throughout the wideband frequency range, high gain, low noise and smaller PCB fabrication. Overall, this LNA could be used for the RF front end application working at 4 – 5GHz.

Faculty of Electronics Engineering, Broadcasting College 1, 136th Quy Luu, Phu Ly, Ha Nam, Viet Nam

[https://www.researchgate.net/publication/303405737\\_High\\_gain\\_low\\_noise\\_amplifier\\_design\\_used\\_for\\_RF\\_front\\_end\\_application](https://www.researchgate.net/publication/303405737_High_gain_low_noise_amplifier_design_used_for_RF_front_end_application)

Low noise amplifier, C band, noise figure, satellite receiver, ADS



## Design of a Broadband Coplanar Waveguide-Fed Antenna Incorporating Organic Solar Cells with 100% Insolation for Ku Band Satellite Communication

A broadband coplanar waveguide (CPW)-fed monopole antenna based on conventional CPW-fed integration with an organic solar cell (OSC) of 100% insolation is suggested for Ku band satellite communication. The proposed configuration was designed to allow for 100% insolation of the OSC, thereby improving the performance of the antenna. The device structure was fabricated using a Leiterplatten-Kopierfrasen (LPKF) prototyping Printed circuit board (PCB) machine, while a vector network analyzer was utilized to measure the return loss. The simulated results demonstrated that the proposed antenna was able to cover an interesting operating frequency band from 11.7 to 12.22

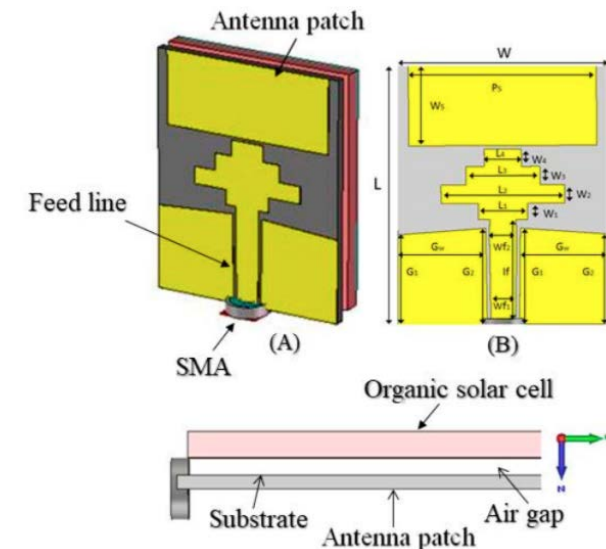
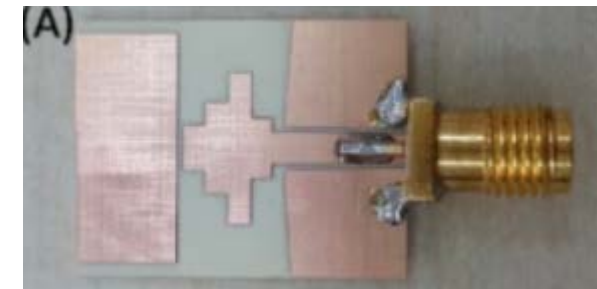
### Fabrication and Measurement of the Proposed Antenna

The antenna structure was fabricated by using a E33 model LPKF prototyping PCB machine at Department of Electrical and Electronics, Iskenderun Technical University, Hatay, Turkey. In our research work, we had a chance to only fabricate the proposed antennas without organic solar cell due to the instrumentation limitation in our labs. A single sided copper covered the IS680 substrate with a thickness of 0.762 mm chosen in the manufacturing process for the proposed antenna. After the fabrication of the antenna, a 50 Ω SMA connector was soldered to the feeding line and ground plane, as illustrated in Figure 3.

School of Physics and Electronics, Central South University, Changsha 410083, China

<https://www.mdpi.com/1996-1944/13/1/142/htm>

Ku Band, coplanar waveguide, organic solar cells



## A Low-Profile Antenna Based on Single-Layer Metasurface for Ku-Band Applications

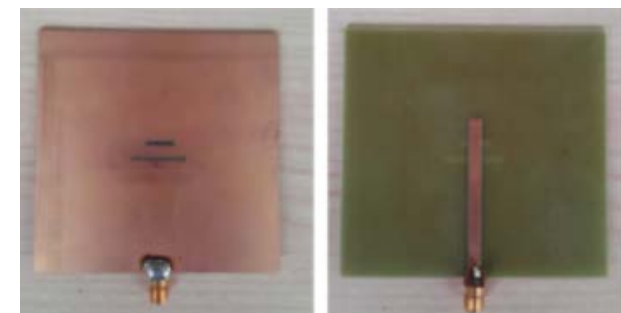
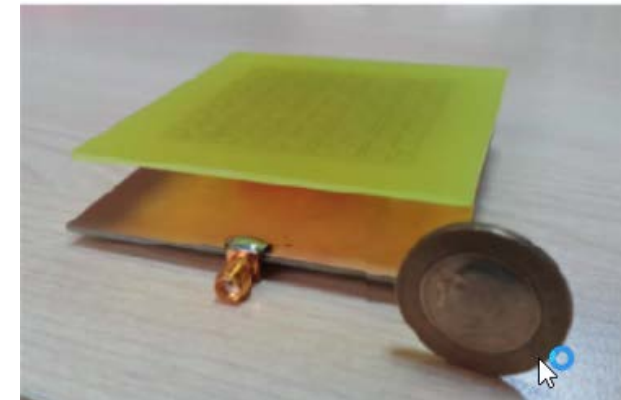
Improvement in the antenna gain is usually achieved at the expense of bandwidth and vice versa. This is where the realization of this enhancement can be made through compromising the antenna profile. In this work, we propose a new design of incorporating periodic metasurface array to enhance the bandwidth and gain while keeping the antenna to a low-profile scheme. The proposed antenna was simulated and fabricated in order to validate the results in the operating frequency range from 10 MHz to 43.5 GHz. Computer simulation technology (CST) microwave studio software was used to design and simulate the proposed antenna, while LPKF prototyping PCB machine was utilized to fabricate the antenna. Results showed that the antenna generated a gain and bandwidth of 14.2 dB and 2.13 GHz, respectively. Following the good agreement between the numerical and measurement results, it is believed that the proposed antenna can be potentially attractive for the application of satellite communications in Ku-band electromagnetic wave.

The utilization of a single-layer metasurface was successfully proposed to simulate and fabricate a high gain and band-width antenna of a reasonably low-profile scheme. The simulation results from CST microwave studio and HFSS tools were found to be in good agreement with the experimental one. Results showed the presence of three characteristic resonant frequencies of the antenna.

School of Physics and Electronics, Central South University, Changsha, Hunan 410083, China

<https://www.researchgate.net/publication/348193337> A Low-Profile Antenna Based on Single-Layer Metasurface for Ku-Band Applications

patch antenna, metasurface,



## Printed Microwave Metamaterial-Antenna Circuitries on Nickel Oxide Polymerized Palm Fiber Substrates

In this paper, the novelty of exploring the applications of the Iraqi Palm Tree Remnants (IPTTR) mixed with Nickel Oxide Nanoparticles (NONP) hosted in Polyethylene (PE), called INP substrates, is utilized by printing metamaterial (MTM) based high gain microwave antennas on them. The proposed INP substrates are mainly created from pressed flexible organic fibers to suite the ink jet printing technologies. The complex relative constitutive parameters are characterized in terms of permittivity ( $\epsilon$ ) and permeability ( $\mu$ ) within the frequency range from 2 GHz up to 6 GHz using an open end dielectric probe and a T-stub transmission line technique. To validate the feasibility of the ...

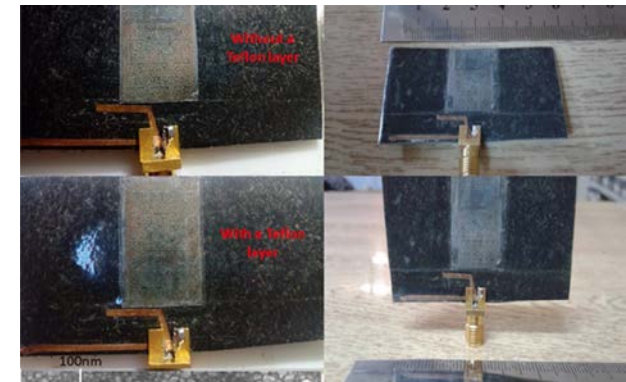
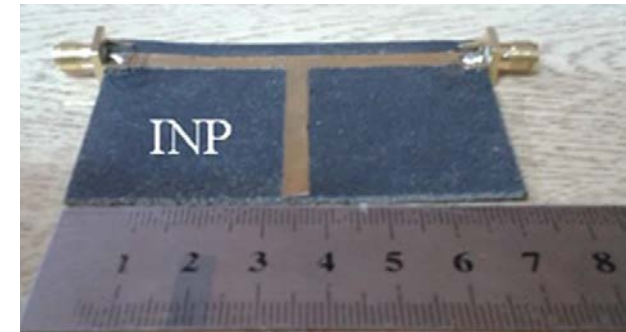
### MTM and dipole antenna structures fabrication

After accomplishing the printing process, an annealing progression inside a ProtoFlow LPKF's convection oven is carried out on the printed surface to avoid oxidization. Nevertheless, the annealing process is invoked to avoid the surface roughness due to the gaps between the nanoparticles. The annealing temperature is fixed at 100 °C for 12 hours to ensure good percolation channels by diminishing potential cracks due toglomeration of the nano structures that lead to conductivity reduction due to the surface roughness as depicted.

Department of Communication Engineering, Al-Mammon University College, Baghdad, Iraq

<https://www.nature.com/articles/s41598-019-39736-8>

Iraqi Palm Tree Remnants (IPTTR),  
Nickel Oxide Nanoparticles (NONP)



## Check for your sources for articles and papers

[www.nature.com](http://www.nature.com)

[www.researchgate.net](http://www.researchgate.net)

[www.mdpi.com](http://www.mdpi.com)

[Springer - International Publisher Science, Technology, Medicine](#)

[Open Access Scientific Reports | OMICS International \(omicsonline.org\)](#)

[LPKF Knowledge center](#)

[Contact LPKF](#)

For any comments to this  
and proposals for next  
report – please click below:



# Publications with LPKF Equipment, Part 2

Selection of internationally published scientific articles using LPKF equipment

May 2021



## TOC: page, system, application

3

[PL S4: Antenna for UHF RFID reader](#)

4

[PL U3: LTCC Microfluidic Devices](#)

5

[PL U4: Implantable flex board](#)

6

[PL U4: Wearable bio-sensor for cerebral monitoring](#)

7

[PL U4: Wearable bio-multisensor](#)

8

[PL U3: Microrollers for in vein drug delivery](#)

9

[PL U4: Wearable microfluidic multisensor](#)

10

[PL U4: Wearable catheter type oximeter](#)

11

[PL U4: 300 GHz antenna for 6G](#)

12

[PL R: Wearable microfluidic biosensors](#)

13

[PL R: Microfluidic strain sensors](#)

14

[PL R: Wearable microfluidic sensors for health care](#)

## An ultra-thin double-functional metasurface patch antenna for UHF RFID applications

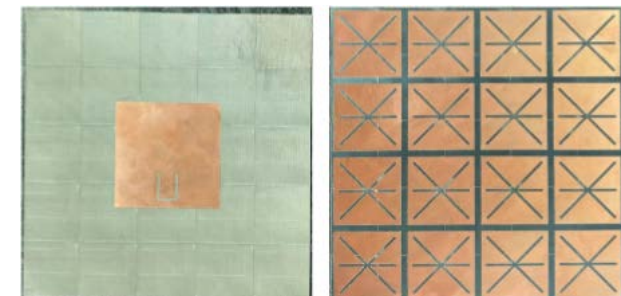
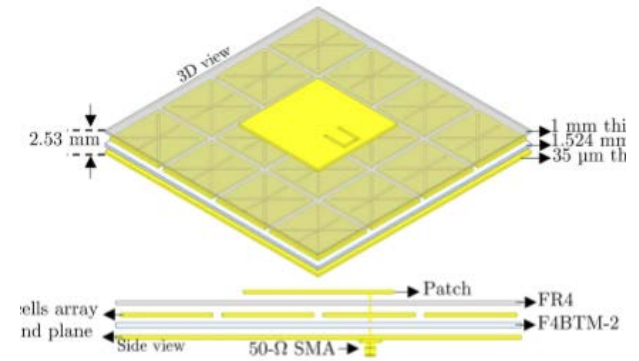
An ultra-thin double-functional metasurface patch antenna (MPA) was proposed, where it can operate not only in the antenna mode but also can simultaneously act as perfect absorber for normal incident waves, suitable for RFID applications in the 868 MHz band. The MPA structure consists of a typical coaxially-fed patch antenna merged, for the first time, with a metasurface absorber acting as artificial ground. A methodology for the unit-cell design of the metasurface is proposed followed by an equivalent circuit model analysis, which makes it possible to transform a low-loss ( $\tan\delta = 0.0015$ ) unit-cell with highly-reflective characteristics to a perfect absorber for ...

The MPA structure proposed in the current study comprises a typical patch antenna (Fig. 1a–d) that its ground plane is substituted with a metasurface absorber structure (Fig. 1b–e). It can be a potential RFID reader as it can operate not only in a normal antenna mode with improved performance but also act as an absorber to suppress scattering, which can effectively reduce the incorrect reading of RFID systems in multipath environment. The patch is printed on a 1-mm-thick inexpensive FR4 epoxy substrate. The metasurface absorber structure composed of 4x4 unit-cell matrix. A laser etching machine (LPKF ProtoLaser S4) was used to realize both the patch and the absorber structures, shown in Fig. 1d,e, respectively. The overall MPA thickness is only 2.53 mm.

Department of Electrical and Control Engineering, École Supérieure d'Électronique de l'Ouest (ESEO), 49107, Angers, France

<https://www.nature.com/articles/s41598-020-79506-5>

metasurface patch antenna (MPA)  
UHF RFID



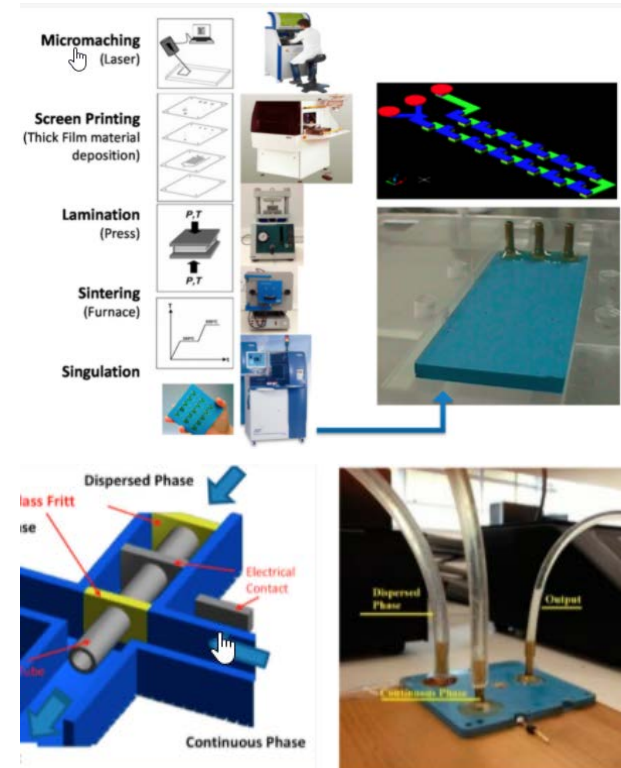
## Fab on a Package: LTCC Microfluidic Devices Applied to Chemical Process Miniaturization

Microfluidics has brought diverse advantages to chemical processes, allowing higher control of reactions and economy of reagents and energy. Low temperature co-fired ceramics (LTCC) have additional advantages as material for fabrication of microfluidic devices, such as high compatibility with chemical reagents with typical average surface roughness of  $0.3154 \mu\text{m}$ , easy scaling, and microfabrication. The conjugation of LTCC technology with microfluidics allows the development of micrometric-sized channels and reactors exploiting the advantages of fast and controlled mixing and heat transfer processes, essential for the synthesis and surface functionalization of nanoparticles.

### LTCC Microfabrication

The microfluidic devices were fabricated employing the LTCC process as shown in Figure 1 (cutting layers, thick film deposition, lamination, sintering, and dicing) [16]. The layers with the microchannel geometries were fabricated using a diode pumped IR laser, model U-15 1064 nm Ultrafast Laser Maker (RMI Laser, LLC, Lafayette, Colo.) and a prototyping machine equipped with an ultraviolet laser (355 nm wavelength), model LPKF ProtoLaser® U3 (LPKF Laser & Electronics AG, Garbsen, Germany). Thermo-compression lamination process is done by means of a uniaxial laminator ...

microfluidic devices; LTCC technology, chemical process intensification



Micromanufacturing Laboratory, Center for Bionanomanufacturing, Institute for Technological Research, 05508-901 São Paulo, Brazil

<https://www.mdpi.com/2072-666X/9/6/285/htm>



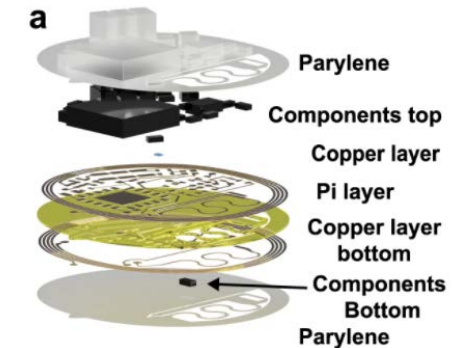
## Wireless battery free fully implantable multimodal recording and neuromodulation tools for songbirds

Wireless battery free and fully implantable tools for the interrogation of the central and peripheral nervous system have quantitatively expanded the capabilities to study mechanistic and circuit level behavior in freely moving rodents. The light weight and small footprint of such devices enables full subdermal implantation that results in the capability to perform studies with minimal impact on subject behavior and yields broad application in a range of experimental paradigms. While these advantages have been successfully proven in rodents that move predominantly in 2D, the full potential of a wireless and battery free device can be harnessed with flying species, where ...

**Device fabrication.** Flex circuits were composed of Pyralux AP8535R substrate. Top and bottom copper layers (17.5  $\mu\text{m}$ ) on a substrate polyimide layer (75  $\mu\text{m}$ ) were defined via direct laser ablation (LPKF U4). Ultrasonic cleaning (Vevor; Commercial Ultrasonic Cleaner 2L) was subsequently carried out for 10 min with flux (Superior Flux and Manufacturing Company; Superior #71) and 2 min with isopropyl alcohol (MG Chemicals) and rinsed in deionized water to remove excess particles. Via connections were manually established with copper wire (100  $\mu\text{m}$ ) and low temperature solder (Chip Quik; TS391LT). Device components were fixed in place with UV-curable glue (Damn Good 20910DGFL) and cured with a UV lamp (24 W) for 10 min. The devices were encapsulated with ...  
Departments of Biomedical Engineering, The University of Arizona, Tucson, AZ, USA.

<https://www.nature.com/articles/s41467-021-22138-8>

wireless, battery-free, fully implantable



## A wireless, skin-interfaced biosensor for cerebral hemodynamic monitoring in pediatric care

The standard of clinical care in many pediatric and neonatal neurocritical care units involves continuous monitoring of cerebral hemodynamics using hard-wired devices that physically adhere to the skin and connect to base stations that commonly mount on an adjacent wall or stand. Risks of iatrogenic skin injuries associated with adhesives that bond such systems to the skin and entanglements of the patients and/or the healthcare professionals with the wires can impede clinical procedures and natural movements that are critical to the care, development, and recovery of pediatric patients. This paper presents a wireless, miniaturized, and mechanically soft, flexible ...

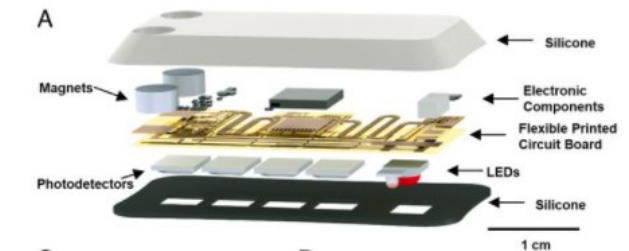
### Device Fabrication

Fabrication began with a 25- $\mu\text{m}$ -thick polyimide sheet, with 12- $\mu\text{m}$ -thick Cu on both sides (AP7164R; Dupont) and outlined using an ultraviolet laser cutter (ProtoLaser U4; LPKF). Electronic and sensor components, along with a pair of magnets (5862K13; McMaster Carr), were bonded to the circuit board by solder paste (TS391LT; Chip Quik). The board was folded and encapsulated within thin layers of medical-grade silicone (Silbione RTV 4420; Elkem) and subsequently filled with soft silicone (Ecoflex 00-10; Smooth-On). The final shape was outlined using a CO2 laser cutter (VLS3.5; Universal Laser).

Querrey Simpson Institute for Bioelectronics, Northwestern University, Chicago, IL 60208

<https://www.pnas.org/content/117/50/31674>

Wearable electronics, near-infrared spectroscopy, bioelectronics, cerebral hemodynamics



## Wireless, soft electronics for rapid, multisensor measurements of hydration levels in healthy and diseased skin

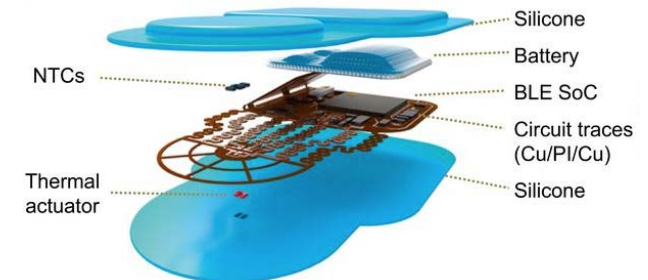
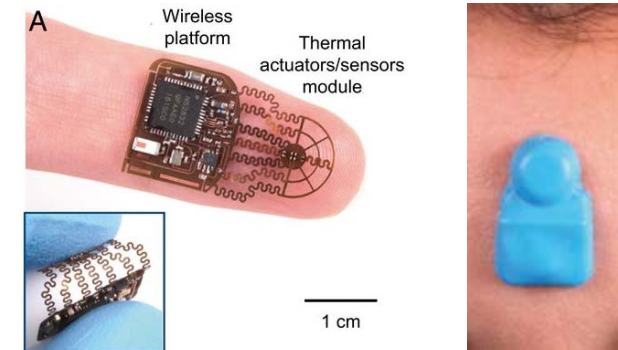
Precise, quantitative measurements of the hydration status of skin can yield important insights into dermatological health and skin structure and function, with additional relevance to essential processes of thermoregulation and other features of basic physiology. Existing tools for determining skin water content exploit surrogate electrical assessments performed with bulky, rigid, and expensive instruments that are difficult to use in a repeatable manner. Recent alternatives exploit thermal measurements using soft wireless devices that adhere gently and noninvasively to the surface of the skin, but with limited operating range (~1 cm) and high sensitivity to subtle ...

### Fabrication of the Electronics.

Prototype devices used flexible copper-clad polyimide substrates (AP8535R; Pyralux) processed by laser ablation (ProtoLaser U4; LPKF), resulting in flexible printed circuit boards (fPCBs) to interconnect surface-mount components, including a BLE SoC (nRF52832; Nordic Semiconductor), resistors (RMCF0201FT; Stackpole Electronics), and temperature sensors (NTC; NCP03XH; Murata). Outcomes of studies of prototype fPCBs served as the basis for designs provided to an ISO-9001 compliant vendor (PCBWay) for final designs. Soldering wire (MM01019; Multicore) and soldering paste (SMDLTLFP10T5; Chip Quik) bonded the BLE SoC to the fPCB by heating at 400 °C, and ...  
Querrey-Simpson Institute for Bioelectronics, Northwestern University, Evanston, IL 60208

<https://www.pnas.org/content/118/5/e2020398118>

Wireless electronics, flexible electronics, bio-medical devices, health monitoring, diagnostics



## Shape anisotropy-governed locomotion of surface microrollers on vessel-like microtopographies against physiological flows

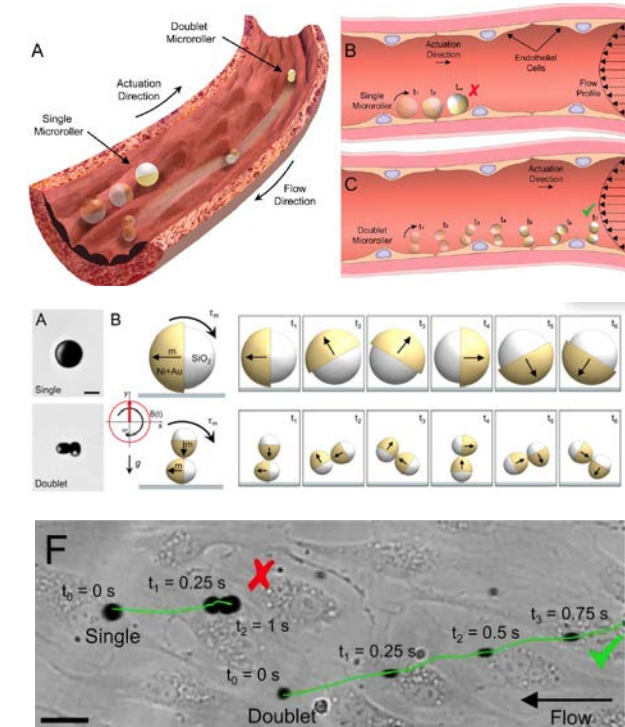
Surface microrollers are promising microrobotic systems for controlled navigation in the circulatory system thanks to their fast speeds and decreased flow velocities at the vessel walls. While surface propulsion on the vessel walls helps minimize the effect of strong fluidic forces, three-dimensional (3D) surface microtopography, comparable to the size scale of a microrobot, due to cellular morphology and organization emerges as a major challenge. Here, we show that microroller shape anisotropy determines the surface locomotion capability of microrollers on vessel-like 3D surface microtopographies against physiological flow conditions.

**Cell Culture Experiments:** For branched endothelialized microfluidic channels, double-sided adhesive tape was micromachined using an ultraviolet laser system (LPKF ProtoLaser U3) with a width of 300  $\mu\text{m}$  for the smallest channel. Human umbilical vein endothelial (HUVEC) cells were grown in endothelial cell growth basal medium 2 (CC-3156, Lonza) supplemented with endothelial cell growth media 2 SingleQuots (CC-4176, Lonza) in a 5% CO<sub>2</sub>, 95% air humidified atmosphere. After reaching to confluence, HUVEC cells were trypsinized and then introduced into the microchannels coated with fibronectin (0.1 mg/mL for 1 h at room temperature) at a concentration of 107 cell/mL and cultured with media flow at 4 dyn/cm<sup>2</sup> for 2 d.

Physical Intelligence Department, Max Planck Institute for Intelligent Systems, 70569 Stuttgart, Germany

<https://www.pnas.org/content/118/13/e2022090118>

Medical robots, surface rollers, circulatory system, microfluidics



## An on-skin platform for wireless monitoring of flow rate, cumulative loss and temperature of sweat in real time

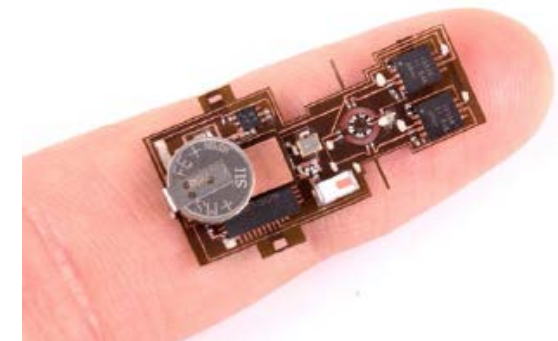
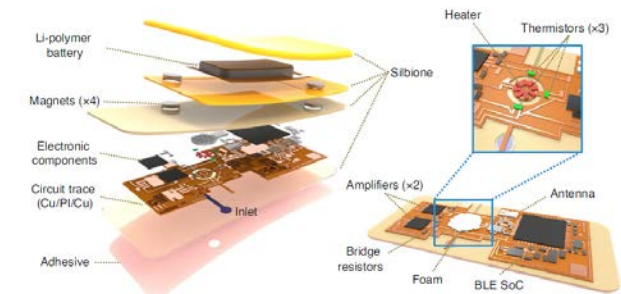
Monitoring the flow rate, cumulative loss and temperature of sweat can provide valuable physiological insights for the diagnosis of thermoregulatory disorders and illnesses related to heat stress. However, obtaining accurate, continuous estimates of these parameters with high temporal resolution remains challenging. Here, we report a platform that can wirelessly measure sweat rate, sweat loss and skin temperature in real time. The approach combines a short, straight fluid passage to capture sweat as it emerges from the skin with a flow sensor that is based on a thermal actuator and precision thermistors, and that is physically isolated from, but thermally coupled to, the sweat.

**Fabrication of the electronics.** A thin, flexible film (AP8535R, Pyralux, DuPont) of copper/PI/copper (thicknesses of 18  $\mu\text{m}$ , 75  $\mu\text{m}$  and 18  $\mu\text{m}$ ) served as a substrate. An ultraviolet laser cutter (Protolaser U4, LPKF) ablated the copper to define conductive traces, bond pads and through-hole vias, resulting in a flexible printed circuit board (fPCB). A silver conductive paint (cat. no. Z05001, SPI Supplies) created conductive plugs between the top and bottom patterned copper layers through the vias when heated at 90 °C using a heat gun (AOYUE Int866). Soldering paste (TS391LT, Chip Quik) was used to join the various surface-mounted components, including the BLE SoC (nRF52832, Nordic Semiconductor), antenna (2450AT18A100, Johanson Technology), amplifier ...

School of Electrical Engineering, Korea Advanced Institute of Science and Technology, Daejeon, Republic of Korea

<http://rogersgroup.northwestern.edu/files/2021/nelectflow.pdf>

Biomedical engineering, health care, microfluidics



## Wireless, implantable catheter-type oximeter designed for cardiac oxygen saturation

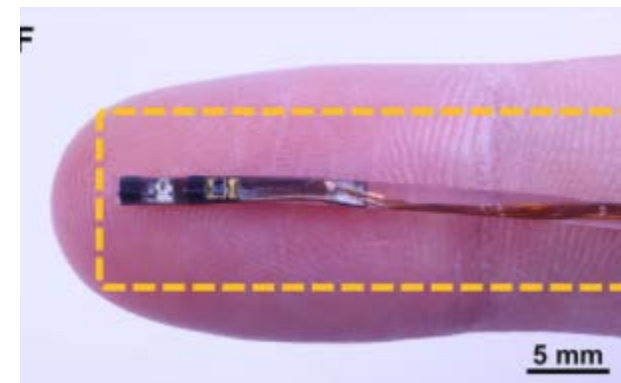
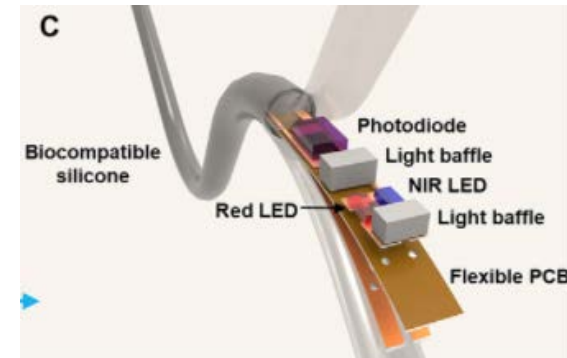
Accurate, real-time monitoring of intravascular oxygen levels is important in tracking the cardiopulmonary health of patients after cardiothoracic surgery. Existing technologies use intravascular placement of glass fiber-optic catheters that pose risks of blood vessel damage, thrombosis, and infection. In addition, physical tethers to power supply systems and data acquisition hardware limit freedom of movement and add clutter to the intensive care unit. This report introduces a wireless, miniaturized, implantable optoelectronic catheter system incorporating optical components on the probe, encapsulated by soft biocompatible materials, as alternative ...

### Fabrication of catheter-type oximeter probe

A flexible sheet of copper-clad polyimide (PI) (Cu/PI/Cu, 18/75/18  $\mu\text{m}$ , AP8535R, Dupont, Pyralux) served as the substrate for the fPCB, with conductive traces, pads, and outline defined by patterned ablation of the copper using an ultraviolet (UV) laser system (ProtoLaser U4, LPKF Co.). The surface mount (SMT) electronic components, red, NIR LEDs, and PD were placed and attached using reflow soldering with low-temperature solder paste (Indalloy 290, Indium Corporation). This electronics module was connected to a detachable connector through four Teflon-coated copper wires (40 AWG enameled copper, Remington Industries) with a length between a few centimeters to 30 cm, ...  
Center for Bio-Integrated Electronics, Northwestern University, Evanston, IL 60208, USA

<https://advances.sciencemag.org/content/7/7/eabe0579>

Health care, implantable sensor, wireless sensor, oximeter



## A 300-GHz low-cost high-gain fully metallic Fabry–Perot cavity antenna for 6G terahertz wireless communications

A low-cost, compact, and high gain Fabry–Perot cavity (FPC) antenna which operates at 300 GHz is presented. The antenna is fabricated using laser-cutting brass technology. The proposed antenna consists of seven metallic layers; a ground layer, an integrated stepped horn element (three-layers), a coupling layer, a cavity layer, and an aperture-frequency selective surface (FSS) layer. The proposed aperture-FSS function acts as a partially reflective surface, contributing to a directive beam radiation. For verification, the proposed sub-terahertz (THz) FPC antenna prototype was developed, fabricated, and measured.

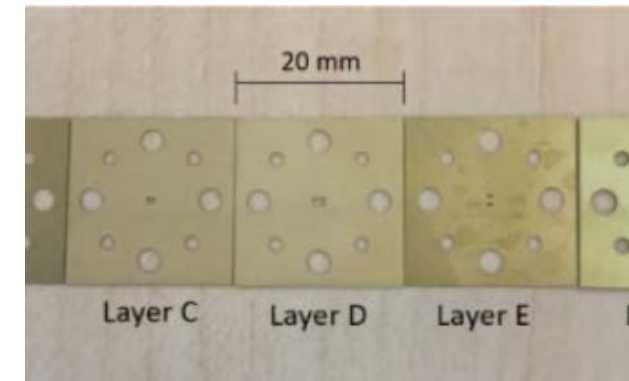
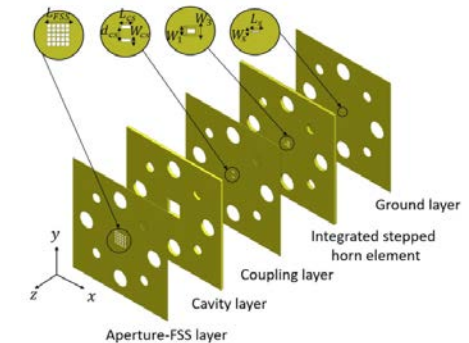
### Fabrication technology

A laser cutting brass technology has been used for each metal layer in the proposed antenna using LPKF ProtoLaser U4 laser machine with technical support from M2ARS (Ch. Guitton and F. Boutet). The seven brass metal layers needed for one antenna assembly, having different thicknesses as shown in Table 1, have been used to manufacture the proposed 300 GHz FPC antenna are shown in Fig. 6a. This brass is often used as a laser-cut metal, which is a highly reflective material. All brass metal layers are fixed by using four plastic screws as shown in Fig. 6. The ultraviolet (UV) laser beam wavelength ( $\lambda = 355$  nm in the UV spectrum), is focused on each brass metal layer individually ...

Institut d'Electronique et des Technologies du numÉrique (IETR), UMR CNRS 6164, Université de Rennes 1, Campus de Beaulieu, 35042, Rennes Cedex, France

<https://www.nature.com/articles/s41598-021-87076-3>

Sub-terahertz , MMW, 6G,



## Skin-Interfaced Microfluidic Systems that Combine Hard and Soft Materials for Demanding Applications in Sweat Capture and Analysis

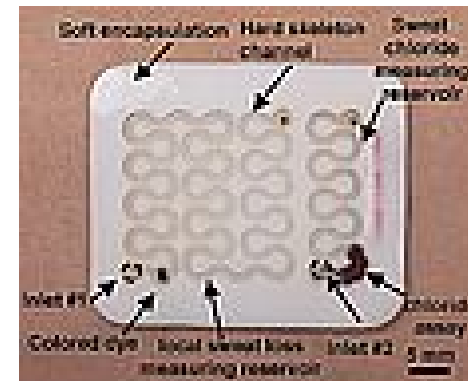
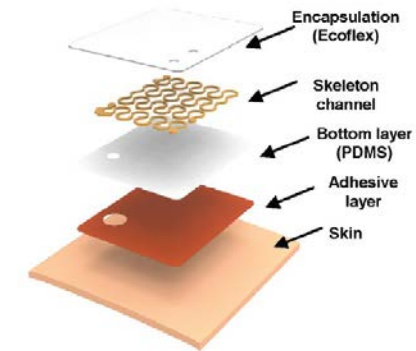
Eccrine sweat contains a rich blend of electrolytes, metabolites, proteins, metal ions, and other biomarkers. Changes in the concentrations of these chemical species can indicate alterations in hydration status and they can also reflect health conditions such as cystic fibrosis, schizophrenia, and depression. Recent advances in soft, skin-interfaced microfluidic systems enable real-time measurement of local sweat loss and sweat biomarker concentrations, with a wide range of applications in healthcare. Uses in certain contexts involve, however, physical impacts on the body that can dynamically deform these platforms, with adverse effects on measurement reliability.

### Fabrication:

... An automated cutting system based on a pulsed laser (LPKF ProtoLaser R, Germany) defined the outline of the serpentine skeletal geometry from the NOA microchannel system. Pouring PDMS(Sylgard 184; Dow corning, MI, USA; mixing ratio of base to curing agent: 10:1) mixed with white silicone dye (Reynolds Advanced Materials) at 10% wt on the PMMA-coated silicon wafer and spin-casting at 300 rpm generated a bottom substrate layer with thickness of 250  $\mu\text{m}$ . Corona treating the NOA skeletal and the white PDMS layer enabled strong bonding between them. Pouring a low modulus silicone precursor (Ecoflex 35) on top after corona treatment, spinning at 150 rpm ...  
School of Mechanical Engineering, Kookmin University, Seoul 02707, Republic of Korea

<http://rogersgroup.northwestern.edu/files/2021/adhmskeleton.pdf>

microfluidic devices, sweat analysis, wearable devices



## Compliant 3D frameworks instrumented with strain sensors for characterization of millimeter-scale engineered muscle tissues

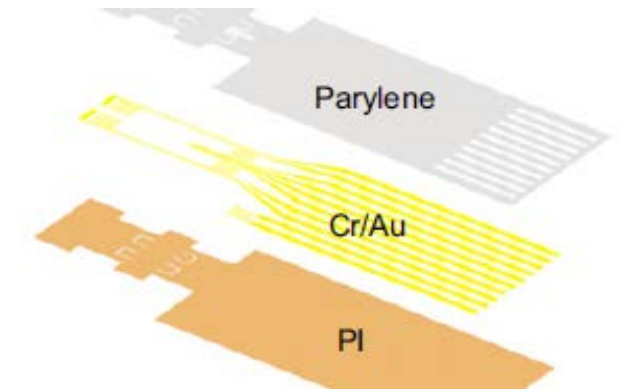
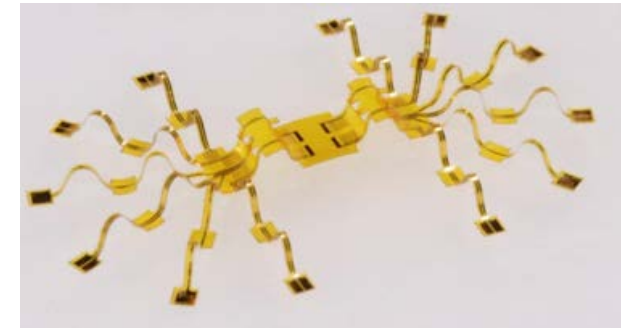
Tissue-on-chip systems represent promising platforms for monitoring and controlling tissue functions in vitro for various purposes in biomedical research. The two-dimensional (2D) layouts of these constructs constrain the types of interactions that can be studied and limit their relevance to three-dimensional (3D) tissues. The development of 3D electronic scaffolds and microphysiological devices with geometries and functions tailored to realistic 3D tissues has the potential to create important possibilities in advanced sensing and control. This study presents classes of compliant 3D frameworks that incorporate microscale strain sensors for high-sensitivity measurements of ...

**Fabrication** of the instrumented 3D frameworks began with spin coating (3,000 rpm for 50 s) a layer of PDMS (10:1 mixing ratio) on a glass slide. Partial curing (90 °C for 60 s) of the PDMS, followed by lamination of a film of PI (12.5 μm in thickness) on top and complete curing (110 °C for 3 min) allowed further processing. A lift-off process defined a patterned metal layer (Cr/Au, 10 nm/100 nm in thickness) on the surface of the PI. Deposition of a layer of parylene C (5 μm) and subsequent patterning using oxygen plasma etching (March RIE) formed a top encapsulation layer. Laser ablation (LPKF ProtoLaser R) defined the outline of the 2D precursor, followed by transfer of the 2D precursor from the PDMS-coated glass to a water-soluble tape (polyvinyl alcohol [PVA]).

Querrey Simpson Institute for Bioelectronics, Northwestern University, Evanston, IL 60208;

<http://rogersgroup.northwestern.edu/files/2021/pnasmuscle.pdf>

three-dimensional electronics, electronic tissue scaffolds, bioelectronics, tissue engineering



## Soft, skin-interfaced microfluidic systems with integrated immunoassays, fluorometric sensors, and impedance measurement capabilities

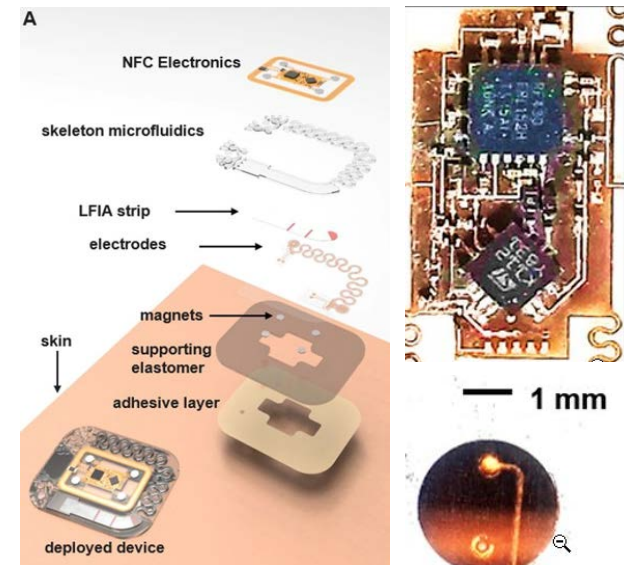
Soft microfluidic systems that capture, store, and perform biomarker analysis of microliter volumes of sweat, in situ, as it emerges from the surface of the skin, represent an emerging class of wearable technology with powerful capabilities that complement those of traditional biophysical sensing devices. Recent work establishes applications in the real-time characterization of sweat dynamics and sweat chemistry in the context of sports performance and healthcare diagnostics. This paper presents a collection of advances in biochemical sensors and microfluidic designs that support multimodal operation in the monitoring of physiological signatures directly correlated to physical ...

**Electronics Design and Assembly:** Fabrication began with patterning of a two-layer printed circuit board by processing of multilayer foils of Cu-PI-Cu (18  $\mu\text{m}$ /75  $\mu\text{m}$ /18  $\mu\text{m}$ ) with a UV laser cutter (ProtoLaser U4; LPKF). The main processor, RF430FRL152HCRGER (RF430, ISO/IEC 15693, ISO/IEC 18000-3; Texas Instruments), served as the NFC platform, with the ability to rectify incident power from a smartphone device at up to 720  $\mu\text{W}$  at 2.0 V, depending on coupling efficiency, and relaying data over the 13.56-MHz communications link. The RF430 supports 14-bit Sigma-Delta ADC with triple analog inputs at an input range up to 900 mV and maximum sampling frequency of 2 kHz, down-sampled to 1-Hz resolution. Signal amplification and measurement of the main and ...

Querrey Simpson Institute for Bioelectronics, Northwestern University, Evanston, IL 60208

<https://www.pnas.org/content/117/45/27906>

Healthcare, soft materials, epidermal devices, sweat cortisol



## Check for your sources for articles and papers

[www.nature.com](http://www.nature.com)

[www.researchgate.net](http://www.researchgate.net)

[www.mdpi.com](http://www.mdpi.com)

[www.pnas.org](http://www.pnas.org)

<https://advances.sciencemag.org/>

[Springer - International Publisher Science, Technology, Medicine](#)

[Open Access Scientific Reports | OMICS International \(omicsonline.org\)](#)

[LPKF Knowledge center](#)

[Contact LPKF](#)